energyequipsys/ Vol 1/2013 / 5-18

Energy Equipment and Systems

www.energyequipsys.com

Film cooling effectiveness in single row of holes: First moment closure modeling

F. Bazdidi-Tehrani [a*]
H. Foroutan
M. Rajabi-Zargarabadi

[a] School of Mechanical Engineering
Iran University of Science and
Technology, Tehran 16846-13114, Iran

Article history:

Received 2 February 2013
Accepted 27 February 2013

ABSTRACT

The present article focuses on the evaluation of a first-moment closure model applicable to film cooling flow and heat transfer computations. The present first-moment closure model consists of a higher level of turbulent heat flux modeling in which two additional transport equations for temperature variance k_θ and its dissipation rate ε_θ are considered. It not only employs a time scale that is characteristic of the turbulent momentum field, but also an additional time scale devoted to the turbulent thermal field. The low Reynolds number k-ε turbulence model is combined with a two-equation k_θ-ε_θ heat flux model to simulate the flow and heat transfer in a three-dimensional single row of cylindrical holes film cooling application. Comparisons with available experimental data show that the two-equation heat flux model improves the over-predictions of center-line film cooling effectiveness caused by the standard simple eddy diffusivity (SED) model with a fixed value of turbulent Prandtl number. This is due to the enhancement of turbulent heat flux components in the first-moment closure simulations. Also, the span wise distributions of effectiveness are computed with more accuracy due to better predictions of coolant jet spreading. However, the limitations of first-moment closure due to its isotropic approach should be taken into consideration.

Keywords: Film Cooling, First-Moment Closure, Two-Equation k_θ-ε_θ Heat Flux Model, Turbulent Heat Flux Modeling.

1. Introduction

Ever increasing turbine inlet temperatures are required so as to achieve higher cycle efficiency in modern gas turbines. However, enhancing the thermal performance of gas turbines by increasing the turbine inlet temperature may cause irreparable damage to the blades. Despite a noticeable progress made in the blade metallurgy, a reasonable lifetime of turbine blades can only be achieved by an efficient surface cooling mechanism such as film cooling. Film cooling is one of the most effective and widely used cooling methods applied to modern gas turbine engines for cooling hot sections such as nozzle vanes and turbine blades.

The working principle of the film cooling is to inject a secondary fluid (coolant) through the holes on a surface, in order to form an air film with lower temperature between the surface and the mainstream which protects the surface from overheating. This technique indeed offers an excellent compromise between the protection of a surface and aerodynamic efficiency. Since, in contrast to convective blade cooling, it minimizes the thermal loads on other components of the turbine. This technique may, however, constitute a source of overall power output loss since the cooling air has to be extracted from the compressor. Thus, optimum film cooling utilizing a minimum amount of cooling air is a major economical requirement. Increasingly, designers are trying to facilitate a greater cooling performance from less coolant air.

Making significant advances in the cooling technology requires a fundamental understanding of the physical mechanisms involved in film cooling flow fields.

*Corresponding author:
School of Mechanical Engineering, Iran University of Science and Technology, Tehran 16846-13114, Iran
E-mail address: bazdid@iust.ac.ir, (F. Bazdidi-Tehrani)

Because of its low-cost, labor-saved and complete data characteristics, the numerical simulation on film cooling investigation is getting more and more important. Along with the rapid development of computational technology, the accuracy of film cooling simulations has improved greatly. Film cooling flow predictions are traditionally carried out employing the Reynolds-Averaged Navier-Stokes (RANS) equations solvers and some turbulence closure models for both velocity and temperature correlations. Therefore, it is important to improve the prediction capabilities of the turbulence models employed in the RANS solutions in order to obtain more reliable information about film cooling characteristics. Turbulent momentum flux closure models employed in film cooling calculations do not generally go beyond the two-equation scope [15]. In the majority of the RANS simulations for film cooling a variety of the k-ε models has been employed to obtain the distribution of eddy viscosity. For instance, Leylek and Zerkle [1994], [17] have used the standard $k-\varepsilon$ model adopting generalized wall functions prescribed by Launder and Spalding [1972], [16].

A detailed analysis of film cooling physics, in a four-part series,has been presented by Walters and Leylek [2000], [23], McGovern and Leylek [2000], [19], Hyams and Leylek [2000],[9], and Brittingham and Leylek [2000], [4], each dealing with different aspects of the film cooling problem. The standard k-ε model employing wall functions and a two layer k-ε model have been utilized by these researchers. The standard and the two layer k-ε turbulence models have also been employed by Lakehal et al. [1998], [14], for investigating film cooling effectiveness of a flat plate comprising a row of laterally injected jets. However, previous simulations of film cooling jets, including those of Lakehal et al. [1998],[14], have shown that the standard two-equation models such as the $k-\varepsilon$ model with wall functions are not adequate for the complex flows, especially when it is needed to investigate heat transfer characteristics. Hoda and Acharya [2000], [8], have conducted a study where various closures for turbulent stresses have been applied for the prediction of coolant jet behavior in a crossflow.

The models taken on ranged from high and low-Reynolds number k-ε and k-ω models to nonlinear eddy viscosity variants. They have stated that the use of high-Reynolds number model in such a complex flow situation is not recommended. Recently, it is shown that attention should also be paid to the strict modeling of turbulent heat flux behavior in the averaged energy equation. However, this is limited to simple flow geometries and most of the publications concerning film cooling of gas turbine components still employ the simple eddy diffusivity (SED) approach for the turbulent heat flux modeling. It has been common to calculate the unknown turbulent heat flux by prescribing a constant turbulent Prandtl number, namely Pr_t=0.9. This value is found experimentally to correspond with the logarithmic region of the boundary layer for flow in a channel. It should not, however, be considered as a universal value since Pr_t is a flow property.

Many experimental and numerical heat transfer studies in the near-wall region have shown that using a constant Pr_t is not adequate for the thermal field predictions. Bazdidi-Tehrani et al. [2008], [3], have investigated the effect of variable turbulent Prandtl number in film cooling heat transfer predictions. They have concluded that it is important to utilize an expression for the turbulent Prandtl number which varies in such a way that it can address the complexity of the film cooling flow properly. Liu et al. [2008], [17], have focused on the influence of Pr_t on the spanwise cooling effectiveness distribution. They have proposed a laterally varying Pr_t, in the form of a table, as a function of lateral location in the jet and the blowing ratio. Lakehal [2002], [12], has employed the TLVA-Pr method, which is a combination of the anisotropic two-layer k-ε turbulence model and the DNS-based model of Pr_t in the boundary layer, in comparison with the isotropic two-layer approach.

He has concluded that with an anisotropic eddy viscosity/diffusivity model the spanwise spreading of the temperature field can well be predicted. Bazdidi-Tehrani and Rajabi-Zargarabadi [2008], [2], have investigated the effects of three different algebraic turbulent heat flux models in combination with the low Reynolds number second moment closure model on the prediction of film cooling characteristics.

They have reported that these models have a significant effect on the prediction of film cooling effectiveness. In the present work, a higher level of turbulent heat flux modeling is developedis not as a remedy for some of the existing models deficiencies, in which two additional transport equations for temperature variance and its dissipation rate are considered. It not only employs a time scale that is characteristic of the turbulent momentum field, but also an additional time scale dedicated to the turbulent thermal field. The combination of a two-equation momentum and a two-equation heat flux closure known as the first-moment closure is widely used in basic flow geometries such as turbulent pipe and channel flow [e.g., Karcz and Badur 2005[10]]. Nevertheless, its application to complex flow and heat transfer processes such as film cooling is seldom addressed. The aim of the present article is to evaluate the first-moment closure model applicable to film cooling flow and heat transfer computations regarding a single row of cylindrical holes.

2. First -Moment Closure

In the present work, it is assumed that the working fluid (air) is incompressible and Newtonian with temperature-dependent fluid properties. The governing transport equations are the continuity, momentum and energy equations. Turbulence effects are taken into account using the eddy viscosity/diffusivity concept. Then the constitutive closures of turbulent momentum and heat fluxes are obtained using the Boussinesq approximation.

Based on the Boussinesq approximation, the Reynolds stress/turbulent heat flux are related to the local velocity/temperature gradients by an eddy viscosity/diffusivity as follows:

$$\overline{u_i u_j} = -\nu_t \frac{\partial U_i}{\partial x_j}, \overline{u_i \theta} = -\alpha_t \frac{\partial \Theta}{\partial x_i} \tag{1}$$

The turbulence scalar quantities (turbulence kinetic energy, k, and its dissipation rate, ε) used to calculate ν_t are determined from the following modeled transport equations, known as the low Reynolds number k-ε model of Chang et al. [1995]:

$$\rho U_i \frac{\partial k}{\partial x_i} = \frac{\partial}{\partial x_i}\left[\left(\mu + \frac{\mu_t}{\sigma_k}\right)\frac{\partial k}{\partial x_i}\right] + \mu_t\left(\frac{\partial U_i}{\partial x_j} + \frac{\partial U_j}{\partial x_i}\right)\frac{\partial U_i}{\partial x_j} - \rho\varepsilon \tag{2}$$

$$\rho U_i \frac{\partial \varepsilon}{\partial x_i} = \frac{\partial}{\partial x_i}\left[\left(\mu + \frac{\mu_t}{\sigma_\varepsilon}\right)\frac{\partial \varepsilon}{\partial x_i}\right] + f_1 C_1 \mu_t \frac{\varepsilon}{k}\left(\frac{\partial U_i}{\partial x_j} + \frac{\partial U_j}{\partial x_i}\right)\frac{\partial U_i}{\partial x_j} - \rho f_2 C_2 \frac{\varepsilon^2}{k} \tag{3}$$

where, C_1, C_2, σ_k and σ_ε are the same empirical turbulence model constants as those conventionally employed in the high Reynolds number k-ε model:

$C_1 = 1.44$, $C_2 = 1.92$, $\sigma_k = 1.0$, $\sigma_\varepsilon = 1.3$

The damping functions, f_1 and f_2, are used to make the low Reynolds number model valid in the near wall region and are defined as follows:

$$f_1 = 1.0$$
$$f_2 = [1 - 0.01\exp(-\mathrm{Re}_t^2)][1 - \exp(-0.0631\mathrm{Re}_y)] \tag{4}$$

where, turbulent Reynolds numbers, Re_t and Re_y, are expressed as in the following equation.

$$\mathrm{Re}_t = \frac{k^2}{\nu\varepsilon}, \quad \mathrm{Re}_y = \frac{\sqrt{k}y}{\nu} \tag{5}$$

The eddy viscosity, ν_t (see Eq.(1)), can be obtained from Eq.(6).

$$\nu_t = C_\mu f_\mu \frac{k^2}{\varepsilon} \tag{6}$$

where, C_μ=0.09 and the empirical function, f_μ is defined as:

$$f_\mu = [1 - \exp(-0.0215\mathrm{Re}_y)]^2\left(1 + \frac{31.66}{\mathrm{Re}_t^{5/4}}\right) \tag{7}$$

When the simple eddy diffusivity (SED) assumption (i.e., using the turbulent Prandtl number) is employed for turbulent thermal field, only the time scale of the fluctuating velocity field, τ, defined as the ratio of turbulence kinetic energy, k, and its dissipation rate, ε (i.e., k/ε) governs both turbulent momentum and heat transfer. In another word, in this approach the eddy diffusivity of heat is expressed in terms of eddy viscosity using the turbulent Prandtl number definition:

$$\alpha_t = \frac{\nu_t}{\mathrm{Pr}_t} \tag{8}$$

The eddy diffusivity of heat should nevertheless be represented as a function of turbulent time scales for both velocity and thermal fields. The turbulent thermal field time scale, τ_θ is the ratio of the fluctuating temperature variance, $k_\theta = \overline{\theta^2}/2$ (where, θ is the fluctuating component of temperature), and its destruction rate ε_θ. Thus the modeling of turbulent heat flux is performed by solving two additional transport equations for k_θ and ε_θ. A two-equation of turbulent heat flux has been successfully implemented by Nagano and Kim [1988], [20], followed by other versions of the $k_\theta - \varepsilon_\theta$ model [e.g., Abe et al. 1995,[1] and Deng et al. 2001,[6]]. The set of governing equations for temperature variance and its destruction rate, based on the Deng et al.'s [2001] proposition is as follows:

$$\frac{Dk_\theta}{Dt} = \frac{\partial}{\partial x_j}\left[\left(\alpha + \frac{\alpha_t}{\sigma_h}\right)\frac{\partial k_\theta}{\partial x_j}\right] - \alpha_t\left(\frac{\partial \Theta}{\partial x_j}\right)^2 - \varepsilon_\theta \tag{9}$$

$$\frac{D\varepsilon_\theta}{Dt} = \frac{\partial}{\partial x_j}\left[\left(\alpha + \frac{\alpha_t}{\sigma_\phi}\right)\frac{\partial \varepsilon_\theta}{\partial x_j}\right] - C_{P1}\sqrt{\frac{\varepsilon\varepsilon_\theta}{2kk_\theta}}\alpha_t\left(\frac{\partial \Theta}{\partial x_j}\right)^2 - C_{d1} f_{d1}\frac{\varepsilon_\theta^2}{2k_\theta} - C_{d2} f_{d2}\frac{\varepsilon\varepsilon_\theta}{k} \tag{10}$$

The relevant model functions and constants are given as in Table 1.

The eddy diffusivity, α_t (refer to Eq.(1)), may be obtained from:

$$\alpha_t = C_\lambda f_\lambda \frac{k^2}{\varepsilon}(2R)^{0.5} \tag{11}$$

where, $R = \tau_\theta/\tau$ is the thermal-mechanical time scale ratio, C_λ=0.1 and

$$f_\lambda = \left[1 - \exp\left(-\frac{\mathrm{Re}_\varepsilon}{16}\right)\right]^2\left[1 + \frac{3}{\mathrm{Re}_t^{3/4}}\right] \tag{12}$$

film hole pitch-to-diameter ratio of P/D=3. The hole length-to-diameter ratio, L/D, is equal to 1.75.

The boundary layer on the flat surface is experimentally determined to be fully turbulent from the leading edge onward, due to a tiny separation bubble located at the flat plate leading edge.

Table 1.Summary of Model Constants and Functions Appearing in $k_\theta - \varepsilon_\theta$ Equations [Deng et al. 2001, [6]]

$\sigma_h = 1.0$	$\sigma_\phi = 1.0$	$C_{P1} = 2.34$	$C_{d1} = 2.0$	$C_{d2} = 0.9$	$C_{\varepsilon 2} = 1.9$	$\mathrm{Re}_\varepsilon = y(\nu\varepsilon)^{1/4}/\nu$
$f_{d1} = \left[1 - \exp\left(-\frac{\mathrm{Re}_\varepsilon}{1.7}\right)^2\right]$		$f_{d2} = \left(\frac{C_{\varepsilon 2} f_\varepsilon - 1}{C_{d2}}\right)\left[1 - \exp\left(-\frac{\mathrm{Re}_\varepsilon}{5.8}\right)^2\right]$			$f_\varepsilon = \left[1 - 0.3\exp\left(-\frac{\mathrm{Re}_t}{6.5}\right)^2\right]$	

The first-moment closure procedure in the form of a flowchart is depicted in Fig.1.

3. Computational Approach

3.1. Problem Description and Boundary Conditions

The three-dimensional test case for the present study is chosen according to the experimental work of Sinha et al. [1991], [22]. As represented by Fig.2 it consists of a single-row of jet holes on a flat surface, with a 35º stream wise injection angle and the coolant fluid is injected from a supply plenum located beneath the flat surface. The coolant mass flow rates are reported to be equal for each of the film holes across a given test section.

The computational domain is extended as 50D×10D×1.5D in the x, y and z directions, respectively. In the streamwise direction (x), the domain extends from the inflow plane located at 19D upstream to outflow plane located at 30D downstream of the injection hole.

In the spanwise direction the domain extends from a plane through the middle of the holes (z/D=0) to a plane at z/D=1.5 in the middle between two injection holes, and symmetry conditions are imposed on these planes. The no-slip and adiabatic conditions are imposed on the walls (i.e., flat surface and plenum walls) and zero gradient conditions are used at the outflow boundary.

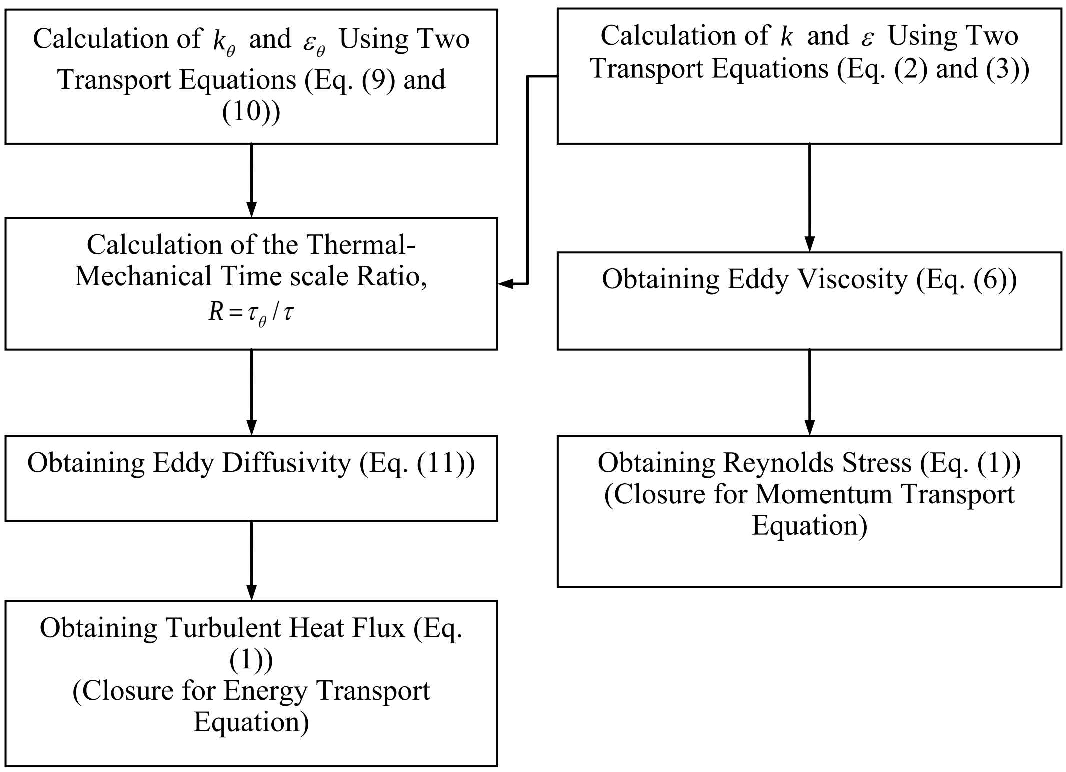

Fig.1. First-moment closure procedure

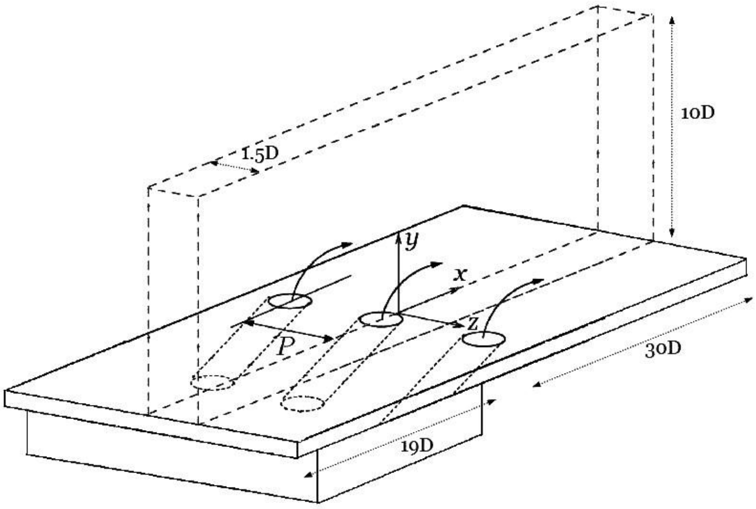

Fig. 2. Schematic of the experimental setup [Sinha et al., 1991, [22]] and computational domain.

The computational extent in the y direction is far enough from the near-field region such that a slip condition with zero normal gradients could be applied on the upper boundary with confidence. The mainstream velocity and temperature are set as $U_\infty = 20$ m/s and $T_\infty = 302$ K, conforming to the experimental set up. Also, uniform distributions are specified for k and ε corresponding to a free-stream turbulence intensity of 0.5% and a dimensionless eddy viscosity of $\nu_t / \nu = 50$ [Lakehal 2002, [13]]. The plenum inlet velocity may be varied so as to impose the required blowing rate, M ($= \rho_j U_j / \rho_\infty U_\infty$, defined as the coolant-to-cross flow ratio of mass flux). For all the computational cases, coolant inlet temperature is set as 153 K, corresponding to a density ratio of approximately 2.0. All other variable quantities for the present work are also matched with the experimental data of Sinha *et al.* [1991], [22].

3.2. Numerical Method

The governing differential transport equations are converted to algebraic equations before being solved numerically. The finite volume scheme which involves integrating the governing equations about each control volume yielding discrete equations that conserve each quantity on a control volume basis is applied. The numerical computations are carried out using the extended version of the CFD code ISAAC 2001,[10], which has been widely validated for different cases [e.g., Morrison et al. 2003, [20] and Bazdidi-Tehrani and Rajabi-Zargarabadi 2008, [2]].

The code is presently extended to comprise the two-equation k_θ-ε_θ model and also compute the development of the components of turbulent heat flux. ISAAC employs a second-order, upwind, finite volume method where viscous terms are discretized by a second-order central difference scheme. Mean and turbulence equations are solved coupled using an implicit spatially split, diagonalized approximate factorization solver.Multi-grid acceleration is applied to the mean flow equations and mesh sequencing (full multi-grid) is employed to provide an initial solution. The computations are terminated when the sum of the absolute residuals normalized by the inflow is less than 10^{-6} for all variables and also the mass-weighted average temperature in the y-z plane at the streamwise position, x/D=10, changes less than 0.1% by increasing iterations.

To resolve the near wall region with large gradients satisfactorily, finer computational grids are set near the wall. For the low Reynolds number models, it is important that the y^+ values of the grid points closest to the wall be of the order of unity. Here, the grid generated is fine enough to reach y^+~1 in the wall adjacent cells.

Computational grid consists of 664,000 body-fitted rectangular cells which has been carefully generated and examined for the grid independence solution. An investigation on the independence of present results from grid size is carried out to determine the appropriate mesh size. Figure 3 represents the effect of grid size on the predicted distribution of center-line film cooling effectiveness, η $(=(T_\infty - T_w)/(T_\infty - T_j)$ where, T_∞, T_w and T_j are mainstream, wall and jet temperatures, respectively). It is evident that the coarse grid size of 362,000 is not appropriate since it causes more than 10% error on average in the present results. The largest difference of the local η between the grid sizes of 497,000 and 664,000 is 3.75%, whereas it is 1.5% between the grid sizes of 664,000 and 800,000. Hence, the mesh size of 664,000 is believed to be sufficiently accurate and (based on the pipe diameter and bulk velocity). The results of computations are presented for a cross section (i.e., 39.9 diameters downstream from the beginning of the test section) where the flow is reported to be fully developed. It is employed throughout the present computations.

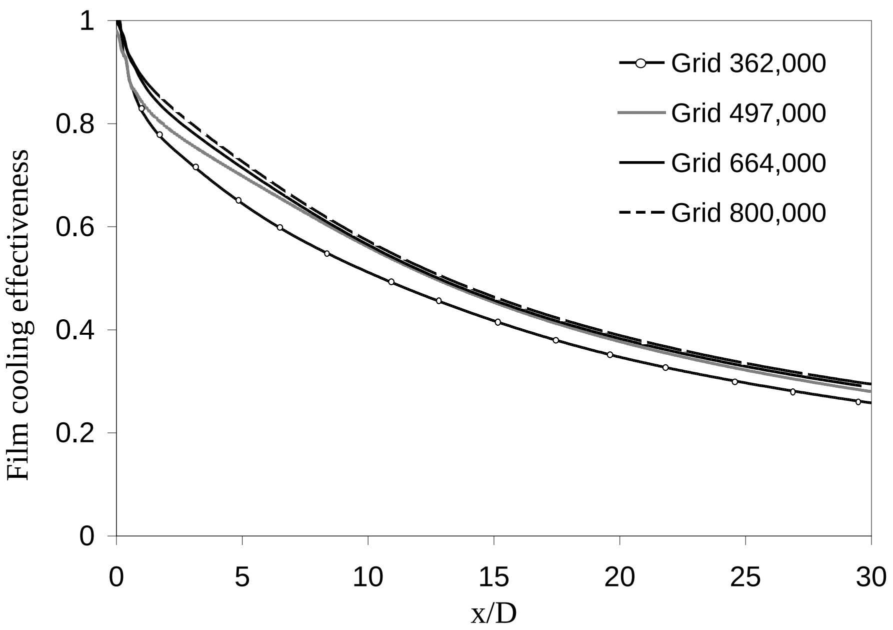

Fig. 3. Effect of grid size on the predicted film cooling effectiveness.

4. Results and Discussion

4.1.Model Validations

In order to validate the present proposed first-moment closure model, it has been applied to a turbulent pipe flow and the characteristics of turbulent heat transfer are also considered. The experimental work of, Hishida and Nagano [1979], [7] comprising a heated pipe by means of a uniform wall temperature, is selected employing air flow at a Reynolds number of Re=40,000 Fig.4 shows the profiles of measured and computed mean temperature, T^+, normalized by the friction temperature in the wall coordinates. The wall coordinates extend from the pipe wall (y^+=0) to near the pipe center-line (y^+=1000). The present computational results are obtained using the first-moment closure model for both flow and thermal fields (i.e., the two-equation $k-\varepsilon$ model for the eddy viscosity and two-equation $k_\theta-\varepsilon_\theta$ model for the thermal eddy diffusivity).

The present profile is reasonably concurrent with the available experimental data of Hishida and Nagano [1979], [7] and the under-prediction caused by applying the SED model (i.e., with a constant prescribed value of Pr_t) is considerably improved. The profiles of normalized temperature variance k_θ^+ are represented by Fig.5. The shape of the present predicted profile is quite similar to that of the experimental data. However, some over-prediction of k_θ^+ value, by 14% on average, is observed. This is also reported in the other computational studies such as Karcz and Badur [2005], [11].

The variations of the production of normalized temperature variance P_θ^+ are depicted in Fig.6. This parameter is defined as (see also Eq.(9)):

$$P_\theta = -\overline{u_i\theta}\frac{\partial\Theta}{\partial x_i} = \alpha_t\left(\frac{\partial\Theta}{\partial x_i}\right)^2 \tag{13}$$

It can be seen that, in line with the results reported in Fig.4 and Fig.5 the present predictions of P_θ^+ are in moderately good agreement with the existing measurements.

4.2. Film Cooling Heat Transfer Calculations

First-moment closure modeling is applied to obtain film cooling heat transfer predictions for a single row of inclined cylindrical holes based on the experimental study of Sinha et al. [1991], [22]. The present computations are carried out for the blowing rate of M=$\rho_j U_j / \rho_\infty U_\infty$=0.5.

Figure 7 illustrates the streamwise variations of center-line film cooling effectiveness, η_c applying both the SED model (i.e., at fixed Pr_t=0.85) and the two-equation k_θ-ε_θ turbulent heat flux model of Deng et al. [6] (i.e., Present). In all cases, the low Reynolds number $k-\varepsilon$ model of Chang et al. [5] is employed for modeling of the flow field. Using the SED model, η_c is shown to be over-predicted in the downstream region (x/D>10) by 18.4% on average, as compared with the available experimental data of Sinha et al. [1991], [22]. In the region near the injection hole (x/D<5), the agreement is marginally improved. Applying the two-equation turbulent heat flux model of Deng et al. [2001] comparatively improves the present predictions of η_c in almost all x/D with a difference of less than 10% on average.

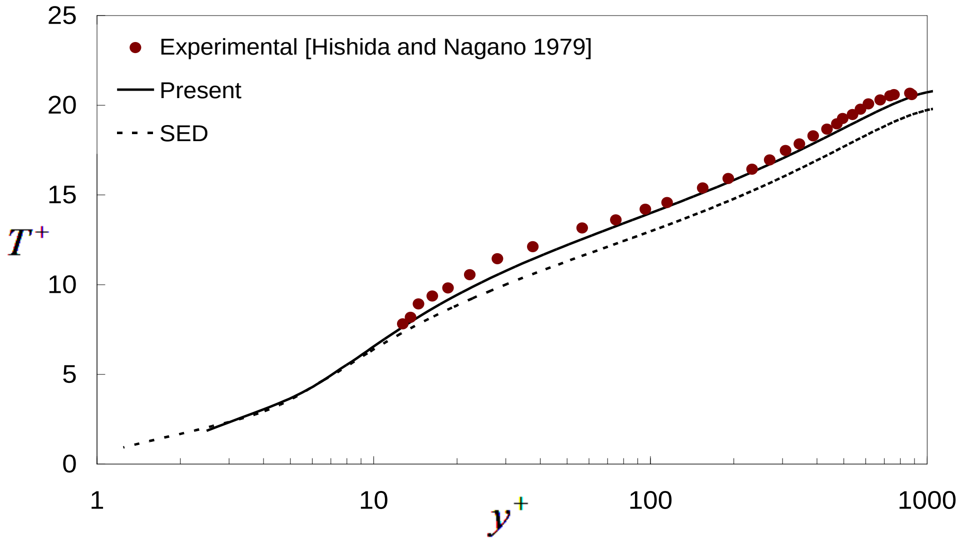

Fig.4. Normalized means temperature profiles in wall coordinates

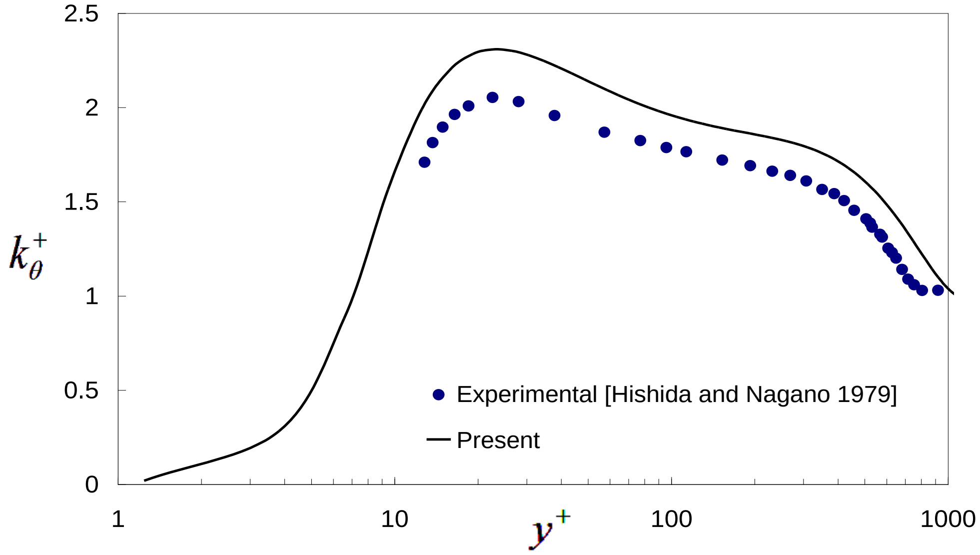

Fig.5. Profiles of normalized temperature variance in wall coordinates

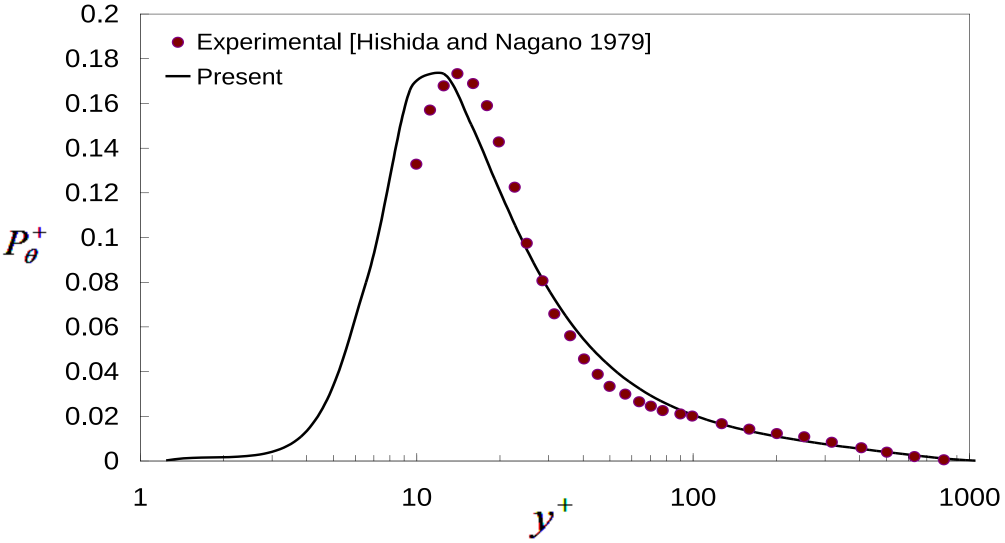

Fig.6. Variations of production of the normalized temperature variance

The results obtained from the present first-moment closure model are in reasonably good agreement with the existing experimental data and also with the TLVA-Pr model of Lakehal [13] (i.e., TLVA-Pr is a combination of the anisotropic two-layer k- ε model and the DNS-based model of Pr_t).Nevertheless, the present model particularly improves the over-prediction observed in the downstream region using the SED model. This is mainly because applying the two-equation heat flux model causes an increase in the predicted components of turbulent heat flux, as discussed in Figures 8-10.This, in turn, results in enhancing the heat transfer between the coolant air and hot mainstream and consequently lower (more realistic) values for η_c .

Figures 8 to 10, depict the present predictions of the streamwise, wall-normal and spanwise distributions of non-dimensional turbulent heat flux, respectively, at the hole center-line plane and for different streamwise locations, x/D. Results are obtained using both the SED and two-equation turbulent heat flux models. As x/D increases, the temperature gradient reduces due to the mixing between the coolant air and the mainstream. Thus, the turbulent heat flux profiles model predicts relatively higher values, because itdecrease (see Eq. (1)) as x/D increases and almost vanish toward the end of the flat plate. Also, for y/D>2 the temperature gradient and hence turbulent heat fluxes are negligible and, thus, all of the profiles are plotted up to the wall normal distance of 2D.

Figure 8 displays the distributions of streamwise component of turbulent heat flux. It has a negative sign near the wall and a positive sign in the outer region. This is due to the fact that the temperature gradient inside the boundary layer in the streamwise direction is positive while it is negative outside. As the boundary layer develops toward the downstream section, the streamwise component remains negative in more extended regions from the wall (i.e., for y/D<0.3 at x/D=1, and y/D<1.1 at x/D=20). Both the SED and present models display similar trends for this component. However, the present first-moment closure model predicts relatively higher values, because it allows higher predictions for the eddy diffusivity in comparison with the SED model which applies a fixed value of $\mathrm{Pr}_t = 0.85$.

The wall-normal component of the turbulent heat flux$\overline{v\theta}$, as represented in Fig.9 is the most important component and it has the maximum magnitude as compared with the other two components. It has a negative sign because of the temperature gradient being positive in the wall-normal direction. Applying the present two-equation turbulent heat flux model increases the value of the wall-normal component relative to the SED, especially near the injection hole (x/D=1). The distributions of the spanwise component of the turbulent heat flux $\overline{w\theta}$, are illustrated in Fig.10. It can be seen that this component is also negative and it is of smaller magnitude as compared with the wall-normal component. This is the result of a lower temperature gradient in the spanwise direction when compared with the wall-normal direction.

The spanwise distributions of film cooling effectiveness η_L , at x/D=1, 3, 6 and 10 are plotted in Fig.11. The predictions by the SED model display significant deviations from the available experimental data. η_L is overestimated at the jet center-line (z/D $\approx$ 0) while it is underestimated at larger z/D.

Also, the present first-moment closure model gives comparatively better results, at various x/D. The distributions of η_L is predicted quite well, especially at z/D<0.5. Applying the two-equation heat flux model results in enhancing the heat diffusion ability, meaning that the lateral heat flux from the jet border to its center is increased and consequently the temperature in the jet center region is increased. In another word, the present model predicts much spreading of the coolant jet in the spanwise direction which is more realistic. The difference between the SED and the present model calculations becomes larger as x/D increases. This is because the coolant jet spreads more as it moves further downstream.

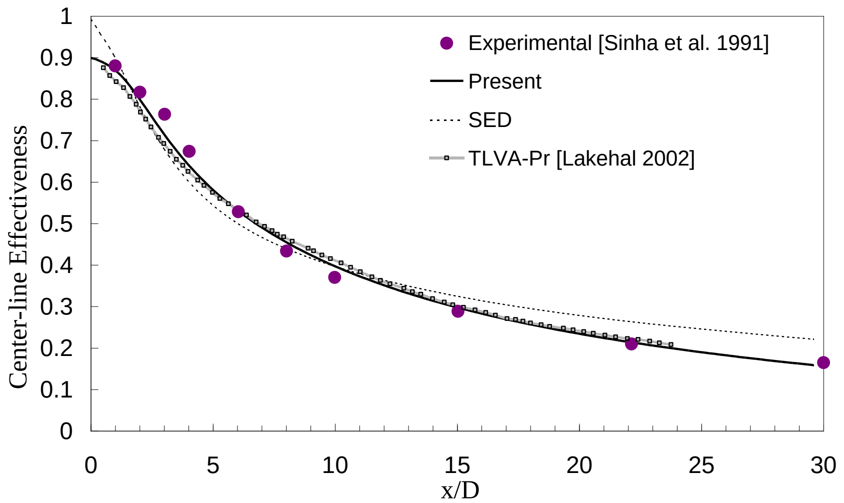

Fig. 7. Streamwise variations of Center-line film cooling effectiveness.

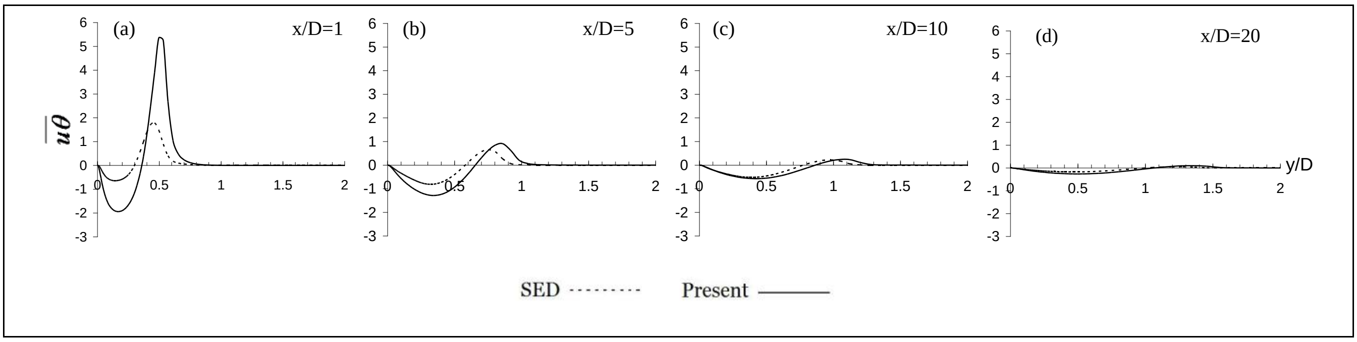

Fig. 8. Streamwise turbulent heat flux distributions at the center-line plane: comparison of SED with the present first-moment closure.

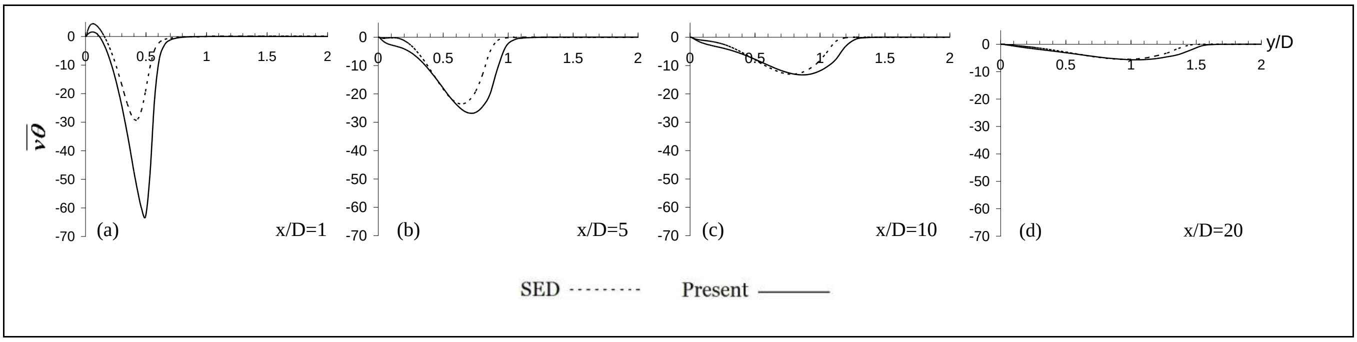

Fig. 9. Wall-normal turbulent heat flux distributions at the center-line plane: comparison of SED with the present first-moment closure.

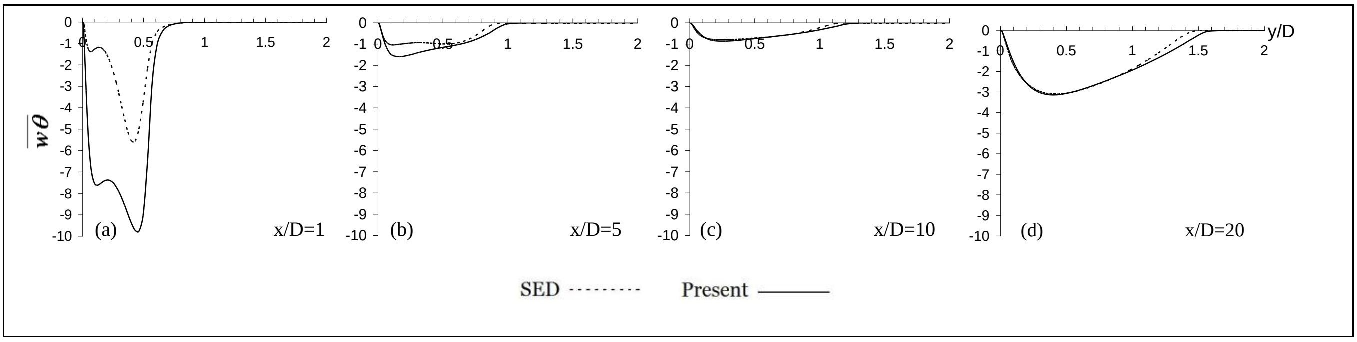

Fig. 10. Spanwise turbulent heat flux distributions at the center-line plane: comparison of SED with the present first-moment closure.

However, it can be seen from Fig.11 that the TLVA-Pr model [Lakehal 2002], which is based on an anisotropic two-layer $k-\varepsilon$ model, gives relatively improved predictions of η_L distributions, particularly at z/D>0.5.

Figure 12 illustrates the predicted temperature contours in the y-z plane and at the axial position, x/D=10. It can be seen that the wall is partly covered by the jet center flow. The jet center temperature predicted by the SED model is noticeably lower than that of the present first-moment closure model in the near wall region. Also, the jet flow temperature behavior becomes distinctly different when moving off the center plane (i.e., as z/D and y/D increase). As discussed in Fig.11 this reflects the predicted pattern of the cooling effectiveness by the present model becoming lower in the center region and then higher at positions off the center-line, as compared with the SED model.

However, it should be noted that there are still deviations between the present model predictions and the available experimental data of Sinha et al. [22] and also the TLVA-Pr model of Lakehal [15], particularly in the lateral region (see, for example, Fig.11d). The main reason for this discrepancy is that the turbulence models and parameters used in the first-moment closure are isotropic and hence they cannot describe the anisotropic nature of the film cooling flow precisely. The Boussinesq approximation employed in Eq.(1) predicts the Reynolds stress/turbulent heat flux based on the mean velocity/temperature gradients alone. In another word, Eq.(1) fails to model the generation of a turbulent heat flux component due to the interaction of turbulent eddies with the mean temperature gradient in the other directions. It is also shown in the film cooling flow [Kaszeta and Simon 2000, [12]] that the eddy viscosity in the spanwise direction is larger than that in the wall-normal direction.

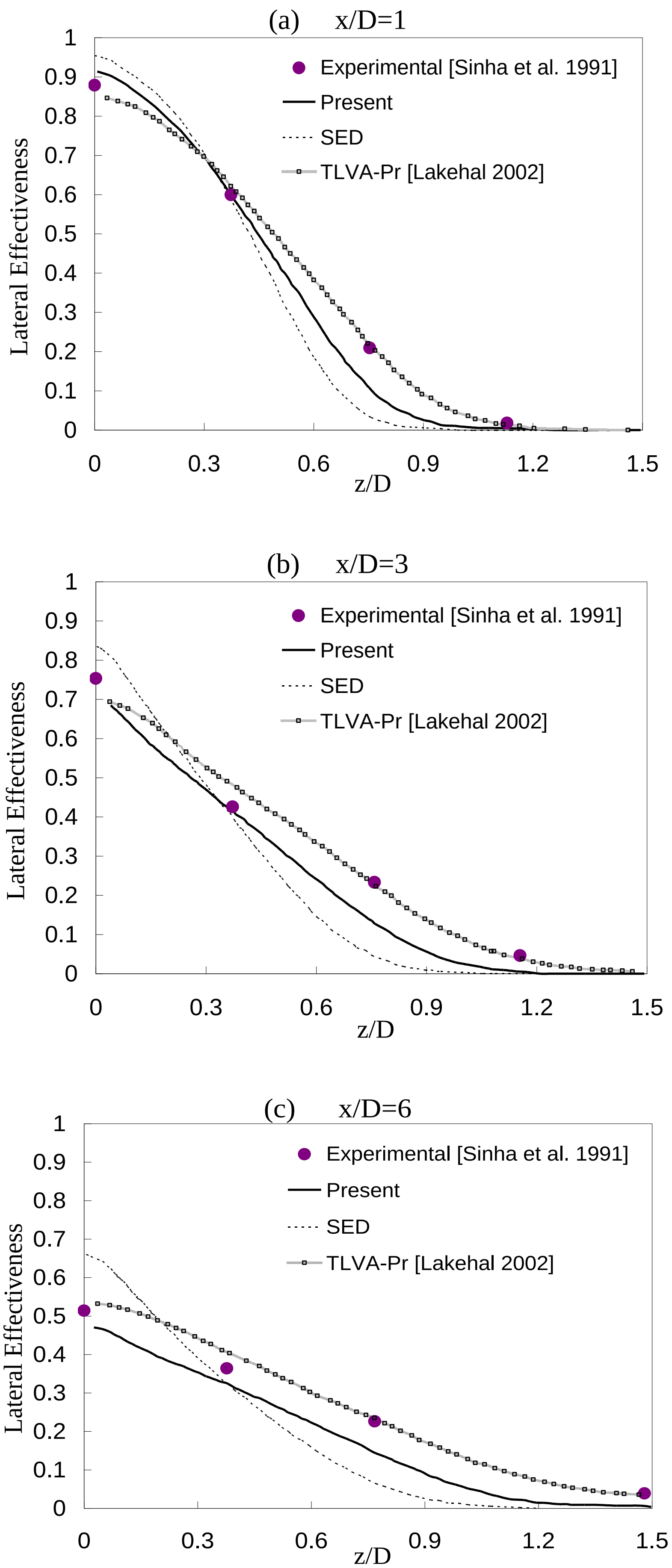
(a) x/D=1
Experimental [Sinha et al. 1991]
Present
SED
TLVA-Pr [Lakehal 2002]
Lateral Effectiveness
z/D
(b) x/D=3
Experimental [Sinha et al. 1991]
Present
SED
TLVA-Pr [Lakehal 2002]
Lateral Effectiveness
z/D
(c) x/D=6
Experimental [Sinha et al. 1991]
Present
SED
TLVA-Pr [Lakehal 2002]
Lateral Effectiveness
z/D

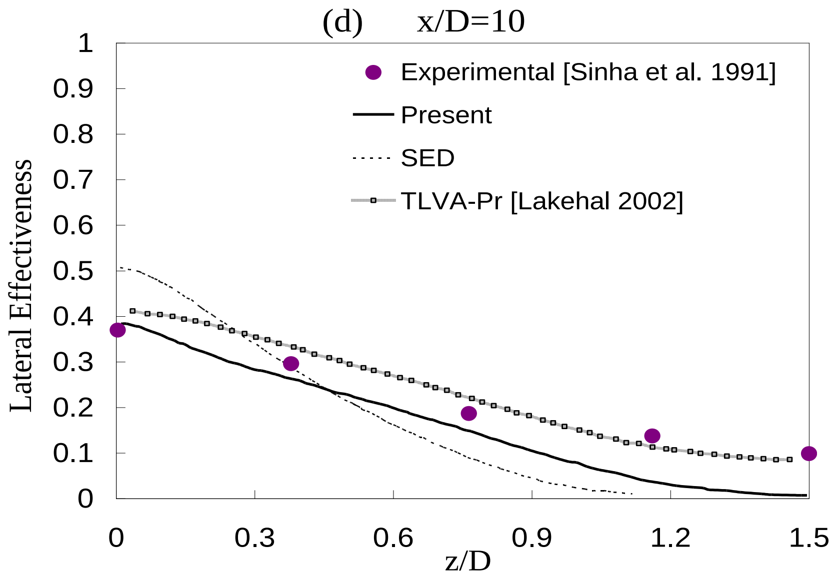

Fig. 11. Spanwise distributions of local film cooling effectiveness.

This cannot be addressed by the isotropic low Reynolds number $k-\varepsilon$ model presently employed. Therefore, more work on the anisotropic models needs to be done for the future development of the film cooling flow and heat transfer models.

5. Conclusions

In the present work, the application of the first-moment closure model to film cooling flow and heat transfer computations is investigated. The low Reynolds number $k-\varepsilon$ turbulence model for flow field is combined with a two-equation $k_\theta-\varepsilon_\theta$ model for thermal field to simulate the flow and heat transfer in a three-dimensional single row film cooling application. The main conclusions are summarized as follows:

(1) In addition to developing turbulence models for flow field, particular attention should also be paid to the precise modeling of turbulent heat flux behavior. Results reveal that the turbulent heat flux model has a significant effect on predicting the thermal field.

(2) Using the simple eddy diffusivity model (SED) with a constant prescribed value of turbulent Prandtl number, the center-line film cooling effectiveness is over-predicted in the downstream region. Applying the two-equation $(k_\theta-\varepsilon_\theta)$

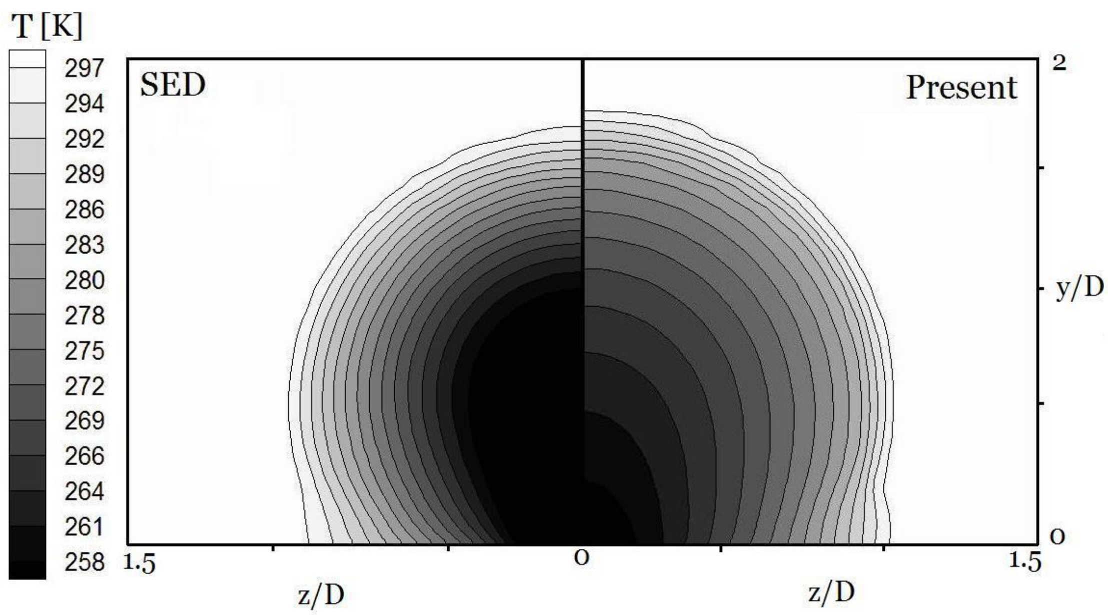

Fig. 12. Temperature contours in the y-z plane, at x/D=10: comparison between SED and present model.

turbulent heat flux model fairly improves the predicted center-line effectiveness. This is mainly because utilizing the two-equation model causes an increase in the predicted turbulent heat flux. This results in enhancing turbulent heat transfer between the coolant air and hot mainstream gas and consequently lower values for film cooling effectiveness.

(3) All components of the turbulent heat flux (streamwise, wall-normal and spanwise) display maximum magnitudes in the near injection-hole region. In the downstream region, due to the mixing of the coolant with mainstream, the temperature gradients and subsequently turbulent heat fluxes almost vanish.

(4) The SED model overestimates the spanwise distribution of film cooling effectiveness at center-line and underestimates it at the location relatively far from it. However, the spanwise distribution is predicted quite well using the first-moment closure model, especially in the region z/D<0.5. Applying the two-equation turbulent heat flux model results in enhancing the heat diffusion ability, meaning that the lateral heat flux from the jet border to its center is increased and consequently the temperature in the jet center region is increased.

(5) Although the first-moment closure is a reliable alternative to the standard constant turbulent Prandtl number concept, it nevertheless has its own limitations. The turbulence models and parameters used in the first-moment closure are isotropic and thus they cannot describe the anisotropic nature of the film cooling flow precisely. More attention to the anisotropic models, both for flow and thermal fields, needs to be paid for film cooling computations.

Nomenclature

D	film-hole diameter
k	turbulence kinetic energy
k_θ	temperature variance
M	blowing ratio ($=\rho_j U_j / \rho_\infty U_\infty$)
P	film-hole pitch
$\Pr_t$	turbulent Prandtl number
q_w	wall heat flux
L	film-hole length
R	thermal-mechanical time scale ratio ($=\tau_\theta / \tau$)
Re_t	turbulent Reynolds number ($=k^2 / \nu\varepsilon$)
Re_y	turbulent Reynolds number ($=\sqrt{k}\, y / \nu$)
Re_ε	turbulent Reynolds number ($=y(\nu\varepsilon)^{1/4} / \nu$)
T	temperature
T^+	normalized temperature
u_τ	friction velocity ($=\sqrt{\tau_w / \rho}$)
U_i	time-averaged velocity component
$\overline{u_i u_j}$	Reynolds stress tensor
$\overline{u_i \theta}$	turbulent heat flux vector
x	streamwise coordinate
y	wall-normal coordinate
y^+	dimensionless distance from wall ($=u_\tau y / \nu$)
z	spanwise coordinate

Greek symbols

α_t	thermal eddy diffusivity
ε	dissipation rate of k
ε_θ	dissipation rate of k_θ
η	film cooling effectiveness ($=(T_\infty - T_w)/(T_\infty - T_j)$)
ν_t	eddy viscosity
Θ	mean temperature
θ	fluctuating component of temperature
θ_τ	friction temperature ($=q_w / \rho c_p u_\tau$)
ρ	fluid density
τ	turbulent mechanical time scale ($=k / \varepsilon$)
τ_w	wall shear stress
τ_θ	turbulent thermal time scale ($=k_\theta / \varepsilon_\theta$)

subscripts

∞	freestream
c	center-line
j	jet
L	lateral
w	wall

References

[1] Abe, K., Kondoh, T. and Nagano, Y. [1995], A New Turbulence Model For Predicting Fluid Flow And Heat Transfer In Separating And Reattaching Flows - II. Thermal Field Calculations, Int. J. Heat mass Transfer, Vol. 38, No. 8, pp. 1467-1481.

[2] Bazdidi-Tehrani, F. and Rajabi-Zargarabadi, M.

[2008], Effect of Turbulent Heat Flux Models on Prediction of Film Cooling characteristics, In Proc. 8th Int. Symp. On Advances in Computational Heat Transfer, Marrakech, Morocco, CHT-08-257.

[3] Bazdidi-Tehrani, F., Foroutan, H. and Rajabi-Zargarabadi, M. [2008], Film Cooling Heat Transfer Predictions: Effects of Variable Turbulent Prandtl Number, *In Proc. 16th Annual Conference of the CFD Society of Canada - CFD2008*, Saskatchewan, Canada.

[4] Brittingham, R.T. and Leylek, J.H. [2000], a Detailed Analysis of Film-Cooling Physics: Part IV - Compound-Angle Injection with Shaped Holes. *J. Turbomachinery*, Vol. 122, pp. 133-145.

[5] Chang, K.C., Hsieh, W.D. and Chen, C.S. [1995], A Modified Low Reynolds Number Turbulence Model Applicable to Recirculating Flow in Pipe Expansion, *Trans. ASME, J. Fluid Engr.*, Vol. 117, pp. 417-423.

[6] Deng, B., Wu, W. and Xi, S. [2001], A Near-wall Two-equation Heat Transfer Model for Wall Turbulent Flows, *Int. J. Heat Mass Transfer*, Vol. 44, pp. 691-698.

[7] Hishida, M. and Nagano, Y. [1979], Structure of Turbulent Velocity and Temperature Fluctuations in Fully Developed Pipe Flow, *ASME J. Heat Transfer*, Vol. 101, pp. 15-22.

[8] Hoda, A. and Acharya, S. [2000], Prediction of Film coolant Jet in Crossflow with Different Turbulence Models, *J. Turbomachinery*, Vol. 122, pp. 1-12.

[9] Hyams, D.G. and Leylek, J.H. [2000], A Detailed Analysis of Film-Cooling Physics: Part III - Streamwise Injection with Shaped Holes, *J. Turbomachinery*, Vol. 122, pp. 122-132.

[10] ISAAC [2001], Integrated Solution Algorithm forarbitrary Configurations (ISAAC), ver. 4.2, NASA Langley Research Center.

[11] Karcz, M. and Badur, J. [2005], An Alternative Two-equation Turbulent Heat Diffusivity Closure, *Int. J. Heat Mass Transfer*, Vol. 48, pp. 2013-2022.

[12] Kaszeta, R.W. and Simon, T.W. [2000], Measurement of Eddy Diffusivity of Momentum in Film Cooling Flows with Streamwise Injection, *ASME J. Turbomachinary*, Vol. 122, pp. 178-183.

[13] Lakehal, D. [2002], Near-Wall Modeling of Turbulent Convective Heat Transport in Film Cooling of Turbine Blades with the Aid of Direct Numerical Simulation Data, *ASME J. Turbomachinary*, Vol. 124, pp. 485-498.

[14] Lakehal, D., Theodoridis, G.S. and Rodi, W. [1998], Computation of Film Cooling of Flat Plate by Lateral Injection from a Row of Holes, Int. J. Heat and Fluid Flow, Vol. 19, pp. 418-430.

[15] Lakehal, D., Theodoridis, G.S. and Rodi, W. [2001], Three-dimensional Flow and Heat Transfer Calculations of Film cooling at the Leading Edge of a Symmetrical Turbine blade model, Int. J. Heat Fluid Flow, Vol. 22, pp. 113-122.

[16] Launder, B.E. and Spalding, D.B. [1972], Lectures in Mathematical Models of Turbulence, Academic Press, London, UK.

[17] Leylek, J.H. and Zerkle, R.D. [1994], Discrete-Jet Film Cooling: A Comparison of Computational Results with Experiments, J. Turbomachinery, Vol. 116, pp. 358-368.

[18] Liu, C.-L., Zhu, H.-R. and Bai J.-T. [2008], Effect of Turbulent Prandtl Number on the Computation of Film- Cooling Effectiveness, Int. J. Heat Mass Transfer, Vol. 51, pp. 6208-6218.

[19] McGovern, K.T. and Leylek, J.H. [2000], A Detailed Analysis of Film-Cooling Physics: Part II - Compound-Angle Injection with Cylindrical Holes, J. Turbomachinery, Vol. 122, pp. 113-121.

[20] Morrison, J.H., Panaras, A.G., Gatski, T.B. and Georgantopoulos, G.A. [2003], Analysis of Extensive Cross-Flow Separation Using Higher-Order RANS Closure Models, AIAA Paper No. 2003-3532, pp. 1-11.

[21] Nagano, Y. and Kim, C. [1988], A Two-Equation Model For Heat Transport In Wall Turbulent Shear Flows, ASME J. Heat Transfer, Vol. 110, pp. 583.

[22] Sinha, A.K., Bogard, D.G. and Crawford, M.E. [1991], Film Cooling Effectiveness Downstream of a Single Row of Holes with Variable Density Ratio, Trans. ASME, J. Turbomachinary, Vol. 113, pp. 442-449.

[23] Walters, D.K. and Leylek, J.H. [2000], A Detailed Analysis of Film-Cooling Physics: Part I - Streamwise Injection with Cylindrical Holes, J. Turbomachinery, Vol. 122, pp. 102-112.